In this section, the SRMA mechanism is used to explain why orbital radii of satellites are related to photon energies in the H_2 spectrum. Consider a protosatellite disk consisting of many colliding atoms or molecules. We focus on collisions that occur near the mid-plane of the disk. The types of atoms or molecules are not determined (nor do they need to be) in this analysis and we simply call them *A, B* and *AB*.

Resonance is established at just certain radii, corresponding to what we call resonance rings, in the protosatellite disk where there is a "match" between disk temperatures and photon energies belonging to photons in a discrete spectrum such as the spectrum of molecular hydrogen. The following model is true for SRMA reactions that contribute to resonance. For this model assume these reactions are viewed from a coordinate system that is in corotation with the gas. Also, the possibility that the source of photons is the protosun is mentioned in subsection 2.2.a. If true, then resonance is most likely initiated during the two time periods during the protoplanet's orbit around the protosun when the protoplanet's equatorial plan is essentially parallel to the direction of the protosun's radiation.

1. SRMA reactions happen in abundance due to the chain reaction that results from the multiplying effect of the additional photon produced with each reaction. Because photons are created at the expense of kinetic energy, the temperature decreases in resonance rings.
2. On average, during a resonant reaction the kinetic energy of *A* equals the kinetic energy of *B* for all resonant reactions. This average energy is proportional to *T* and is called K_{mp} the **most probable kinetic energy** for *A* and *B* in the distribution of energies in the gas. In the present model K_{mp} is taken to be *kT*, where *k* is the Boltzmann constant. More will be said about K_{mp} in Appendix 3.
3. During an SRMA reaction a photon (*hv)* is formed (See Eq. (4)). There are two contributions to the photon's energy. i.e. $E_p = |\Delta K| + \Delta$, where ΔK is the loss of kinetic energy of *A* and *B* due to their collision and association to form the molecule *AB* and Δ is a transition energy that *AB* may undergo as it is being created.
4. In a resonance ring within a protosatellite disk, after the collision the photons (*hv's)* and molecules (*AB's)* move essentially tangent to the ring. This condition ensures that photons continue to cause resonant reactions for long distances until they are no longer within the ring. It also ensures *AB*'s are collecting within a narrow ring at a temperature lower than *T*. The direction of the formed molecules is the same as the direction of the circulating gas. The direction of the resonant photons is parallel or antiparallel to the direction of the circulating gas.
5. Once resonance is initiated it persists even though the temperature in the resonance ring becomes increasing lower. At any gas temperature there are always *A*'s and *B*'s with kinetic energies equal to *kT* where *T* is the temperature when the resonance starts.

In subsection 2.3.c the Mousis (2004) *TD*'s were used to determine the constant $C_1 = 2.315$ K·cm in Eq(3) which is rewritten as Eq. (6) below. Using the above model an theoretical relationship between *T* and E_p for resonance in the disks of Uranus, Jupiter and Neptune is determined in Appendix 3 with the result:

$$T = (hc/k)(E_p - \Delta) \qquad (5)$$

where $hc/k = 1.4388$ K·cm and Δ, is the energy defined in the model above, *h* is Planck's constant and c is the speed of light. Eq. (5) is compared to the empirically determined relationship

$$T = (2.315 \text{ K·cm})(E_p - 3720 \text{ cm}^{-1}), \qquad (6)$$

or $$T = 1.609(hc/k)(E_p - 3720\ \text{cm}^{-1}), \quad (6a)$$

where $1.609(hc/k) = C_1 = 2.315$ K·cm.

We note the reasonable agreement between the multiplying constants (1 and 1.609) on the right sides of Eqs. (5) and (6a). This agreement supports the usefulness of the present model and the technique used to determine C_1. Possibly if the simplifying approximations made in Appendix 3 were relaxed, the agreement would be better. The constant 3720 cm^{-1} in Eq. (6a), corresponding to 0.461 eV, may be helpful in the identification of *A* and *B*.

2.7. The Photon Energy Distribution in Saturn's Protosatellite Disk

The complicated Saturnian ring and satellite system cannot be fit using the H_2 spectrum, and so we turn to the hydrogen atom (*H*) spectrum as an alternative. Again, the origin of the *H* photons is not identified in the present investigation. But as before, perhaps the source of the radiation is the protosun as a T Tauri star (Kwan and Fischer 2011) possibly in a FUor or Exor state (Hartmann, Kenyon and Hartigan 1993). A model similar to the one put forward in this paper is used to investigate the origin of the planets and other satellites of the Sun (Lombardi 2015b). Results of that investigation suggest that the source of the required *H* radiation is the protosun in a FUor or Exor state.

The Rydberg formula gives each transition energy $E_p(n_f, n_i)$ for the hydrogen atom in terms of the principle quantum numbers, n_i and n_f. In the Bohr model these quantum numbers correspond to the initial and final states of the electron for a particular transition. The *H* spectrum contains many series of photon energies (each series corresponds to a different n_f value) with each series possessing a distinct limit $E_p(n_f, \infty)$. As n_i approaches ∞ an edge in the *H* spectrum is also approached. Furthermore, Saturn's broad rings have edges, some of which correspond to such an edge in the spectrum.

The spacing between energies in the *H* spectrum approaches zero as a series limit is approached. And because resonance rings have finite widths, they overlap near edges of Saturn's primordial rings. On the other hand some of Saturn's broad rings have edges that don't correspond to a series limit. As n_i gets smaller the spacing between energies gets larger. Resonance rings overlap less and less until they no longer overlap. Outside this region of overlap is where resonance rings create narrow primordial rings that evolve into satellites.

Assuming the hydrogen spectrum of E_p's creates the key resonances in Saturn's protoplanetary disk, we can determine which E_p is associated with each of the satellites of Saturn by correctly pairing some series limits with certain ring edges. Lombardi (2015a) reports a first attempt at making this association of series limits with ring edges that was somewhat successful from the inner edge of the A ring out to Titan. But it was not able to pair hydrogen E_p's with any satellites or rings orbiting closer to Saturn's surface. The present investigation improves the association of limits and edges and successfully explains the complicated ring and satellite system of Saturn.

Table 6 gives the energies of photons emitted during transitions in the range 617.3-2239.5 cm^{-1}, where energy is in wave numbers (cm^{-1}). In the present model, this range of E_p's is associated with the A and E rings and all the satellites in their vicinity. When the inner edges of the A and E rings of Saturn are associated with the series limits $E_p(7,\infty)$ and $E_p(8,\infty)$ the photons in this range are automatically paired with satellite orbital radii or connected to the A or E rings. These findings lead to the development of a

complete PED that is similar in shape to the PED shown in Fig. 5a for all of Uranus's protosatellite disk. (I.e.both have a dip, a peak and a "tail"). In section 2.8, a TD for Saturn's protosatellite disk is determined that matches a theoretically determined Saturnian disk TD (Mousis, Gautier and Bockelee-Moran 2002) in the "tail" of the TD.

2.7.a. The PED for Saturn's A Ring and Beyond

Table 7 lists the inner and outer edges of the A, G and E rings and satellites from Pan in the A ring to Titan. Hyperion lies just beyond Titan with an orbital inclination and orbital eccentricity that classify it as regular. However it has an irregular shape and it is believed that Hyperion is a remnant of a larger satellite that experienced a catastrophic impact (Farinella, Marzari, and Matteoli 1997). Iapetus is beyond Hyperion and the inclination of its orbital plane is 14.7º. All the other regular satellites of Saturn have inclinations of their planes near 0º. Perhaps Iapetus also experienced an impact or it was captured. Hyperion and Iapetus are not included in the present analysis.

Table 6. Photon energies ($E_p(n_f n_i)$) in the hydrogen spectrum used to construct Table 7 and Fig. 12. E_p's are in units of cm^{-1}. Bolded E_p's are in the range 617.3-2239.5 cm^{-1}. n_f and n_i are defined in section 2.7.

n_i	$n_f = 4$	[*i*]	$n_f = 5$	[*i*]	$n_f = 6$	[*i*]	$n_f = 7$	[*i*]	$n_f = 8$
5	(High E_p's)		x		x		x		x
6	↓	[15]	***1341.2***		x		x		x
7		[2]	***2149.9***	[18]	***808.7***		x		x
8			(High E_p's)	[15]	***1333.6***		524.9		x
9			↓	[11]	***1693.5***	[17]	***884.8***		359.9
10				[4]	***1950.9***	[16]	***1142.2***	[19]	***617.3***
11				[2]	***2141.3***	[15]	***1332.6***	[18]	***807.7***
12					(High E_p's)	[14]	***1477.5***	E ring	952.6
13					↓	[13]	**1590.2**	E ring	1065.3
14						[12]	***1679.6***	E ring	1154.8
15						[9]	***1751.8***	E ring	1226.9
16						[8]	***1810.9***	E ring	1286.0
17						[7]	***1859.8***	E ring	1334.9
18						[6]	***1900.8***	E ring	1375.9
19						[5]	***1935.6***	E ring	1410.7
20						A ring&[3][1]	***1965.2***	E ring	1440.3
21						A ring	1990.7	E ring	1465.8
22						A ring	2012.8	E ring	1487.9
23						A ring	2032.1	E ring	1507.2
24						A ring	2049.0	E ring	1524.1
25						A ring	2064.0	E ring	1539.1
↓							↓		↓
∞						IE A[1]	***2239.5***	IE E[10]	***1714.6***

IE stands for Inner Edge.

Bolded E_p's are assigned to individual satellites and ring inner edges in Saturn's satellite system.

Generally unbolded E_p's contributed to the creation of the A ring and E ring. IE A is inner edge A ring.

A satellite index [*i*] to the left of each bolded E_p is assigned to a satellite or ring edge in Table 7.

All unbolded close E_p's contribute to either the A or E ring of Saturn.

[1]Daphnis (E_p(7,20),[3]) is in the Keeler Gap near the outer edge of the A ring. NASA(2021)

E_p(7,8) and E_p(8,9) are out of the range of interest.

(High E_p's) is indicated for many E_p's because they are out of range of interest.

E_p's corresponding to $n_f = 9$ or larger are not included. Apparently they did not create resonance.

Table 7. Photon energies (E_P's) and orbital radii (r/R_s) used for the construction of Fig. 12. The individual pairings of E_p's and r/R_s's are determined by first pairing Ep(7,∞) and Ep(8,∞) with the inner radii of the A and E rings respectively. Then the other pairings automatically fall into place.

Satellite or Ring Edge Name	$[i]$[a]	r/R_s [b]	n_f, n_i [c]	$E_p(n_f, n_i)$ [c] (cm^{-1})
Inner Edge A ring	[1]	2.030	7,∞	2239.5
Pan in Encke Gap	[2]		5,7	2149.9
Pan in Encke Gap	[2]		6,11	2141.4
Average of Pan E_p's	[2]	2.217		2145.7
Daphnis in Keeler Gap	[3]	2.265	7,20	1965.2
Outer Edge A ring		2.270		
Atlas	[4]	2.284	6,10	1950.9
Prometheus	[5]	2.312	7,19	1935.6
F ring	[6]	2.320	7,18	1900.8
Pandora	[7]	2.351	7,17	1859.8
Epimetheus and Janus	[8]	2.511	7,16	1810.9
Inner Edge G ring		2.754		
Aegaeon	[9]	2.779	7,15	1751.8
Outer Edge G ring		2.871		
Inner Edge E ring	[10]	2.987	8,∞	1714.6
Mimas	[11]	3.073	6,9	1693.5
Methone	[12]	3.219	7,14	1679.6
Anthe	[13]	3.280	7,13	1590.2
Pallene	[14]	3.501	7,12	1477.5
Enceladus	[15]		5,6	1341.2
Enceladus	[15]		6,8	1333.6
Enceladus	[15]		7,11	1332.6
Average of Enceladus E_p's	[15]	3.949		1335.8
Tethys, Calypso & Telesto	[16]	4.889	7,10	1142.2
Dione, Helene & Polydeuces	[17]	6.262	7,9	884.8
Outer Edge E ring		7.964		
Rhea	[18]		6,7	808.7
Rhea	[18]		8,11	807.7
Average of Rhea E_p's	[18]	8.745		808.2
Titan	[19]	20.273	8,10	617.3

[a] The satellite indices ($[i]$ values) are assigned to satellites in this table and used in Table 6 and Fig. 12.

[b] Orbital radii in units of the equatorial radius of Saturn. NASA(2021) These orbital radii are transformed with Eq. (8) to give $(r/R_s)'$ values used in Figs. (17) and (18).

[c] The quantum numbers that define transitions in the hydrogen atom and photon energies associated with these transition.

In Table 6 the $n_f = 7$ and $n_f = 8$ series contain close unbolded E_p's where n_i is large at or near the series limits $E_p(7,\infty)$ and $E_p(8,\infty)$. In these regions resonance rings overlap each other and create a broad circular ring where resonance occurs thus laying the ground work for the A and E rings of Saturn. The outer edge of the E ring corresponds to where resonance rings no longer overlap between $E_p(8,11)$ and $E_p(8,12)$. The energy $E_p(8,11)$ corresponds to the first satellite outside the E ring where the resonance ring was not wide enough to overlap an adjacent resonance ring. This satellite is Rhea ([i] = 18). The bolded E_p's at the very bottom of these columns are the series limits $E_p(7,\infty) = 2239.5$ and $E_p(8,\infty) = 1714.6$ cm^{-1}. These limits and the indices, [1] and [10], are associated with the inner edges of the A ring and E ring respectively. The G rings inner edge is not associated with a series limit. Its existence is likely related to an arc of debris that exists near the orbit of the satellite Aegaeon (Hedman et al. 2007a).

In Table 7 the r/R_s values are the orbital radii of satellites and ring edges in units of R_s the equatorial radius (60,268 km) of Saturn. Except for the outer edges of the A and E rings and the inner and outer edges of the G ring, these features are each assigned a satellite index [i]. All together there are 23 bolded E_p's in Table 6. The close E_p's for [i] = 2 (Pan) are averaged as shown in Table 7. The same procedure holds for [i] = 15 and 18. With close E_p's accounted for, the satellite indices range from [1] to [19]. This number of indices accommodates the 19 satellites and ring inner edges (not including the G rings inner edge) from the inner edge of the A ring to Titan. In Tables 6 and 7, notice the outer edge of the A ring occurs very close to the orbital radius of Daphnis with $E_p = E_p(7,20)$. There are no E_p values listed in Table 7 between $E_p(7,20)$ and $E_p(7,\infty)$ because the all are within the A ring. On the other hand outside the A ring E_p values from $E_p(7,20)$ to $E_p(7,9)$ are all assigned to satellites or the narrow F ring. A similar result can be seen for the E ring. But then interestingly all the remaining satellites in the region are accommodated by other E_p's belonging to other series with out any leftover E_p's or leftover satellites. This is a major success of the recent model.

Fig. 12. The Photon Energy Distribution in Saturn's Protosatellite disk for the A ring and beyond

Figure 12

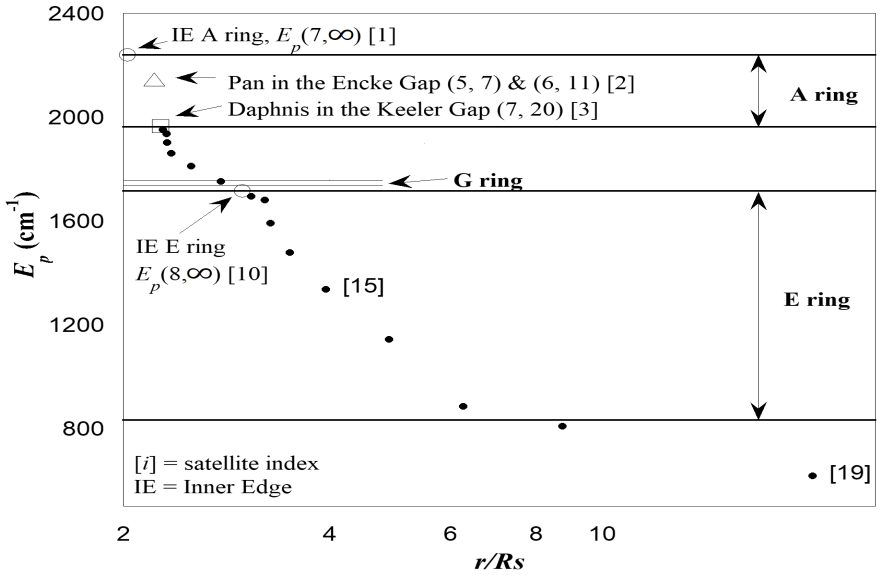

In Table 6 consider $E_p(8,10) = 617.3$ cm^{-1}. This is the lowest E_p value that is bolded, that is assigned to a satellite or inner ring edge. It has satellite index [19] and is associated with Titan. At the top of the $n_f = 7$ and $n_f = 8$ columns, there are two unbolded E_p's that are less than $E_p(8,10)$. If there were two more regular satellites beyond Titan to be considered, they would be associated with these E_p's. There are many E_p's that are indicated in Table 6 as "(High E_p's)" because they are all larger than $E_p(7,\infty) = 2239.5$ cm^{-1} which is the upper range of E_p's included in Table 7.

Fig. 12 is constructed using the data in Table 7. This figure is the PED for Saturn's protosatellite disk from the inner edge of the A ring out to Titan. Notice that the PED consists of two relatively smooth curves that meet at a corner just outside the inner edge of the E ring. This corner plays a critical role in section 2.8 in the determination of the relationship between Saturnian disk PED and TD.

2.7.b. The PED for Saturn's D, C and A Rings

Now consider the PED for Saturn's protoplanetary disk from the inner edge of the D ring out to the outer edge of the A ring. To proceed we explore the possibility that Saturn's disk PED has the same general shape close to Saturn's surface as does Uranus's disk PED close to Uranus's surface. I.e. its shape contains a dip and a peak similar to what are seen in Figs. 5a and 5b. If it does, then some particular E_p's could contribute to Saturn's disk PED up to three times. For this reason it is useful to study the photograph "Panoramic scan across Saturn's rings" (Planetary Society 2021). This scan has labels on distinct gaps in Saturn's rings. Take notice of the similar appearance of the Colombo, Maxwell and Encke Gaps. These three gaps are among the six widest gaps within Saturn's rings. The other three are in the Cassini Division (Planetary Society 2021). The Titan ringlet, Maxwell ringlet and Pan are between the boundaries of each gap respectively (NASA 2021). These similarities lead to the assignment of the same E_p's to the two ringlets as is already assigned to Pan with index [2] in Table 7. To better see this, consider the set of indices [2,23,24] in two places in Tables 8 and the indices [2], [23] and [24] in Table 9. Each of the two ringlets and Pan are associated with *two* closely spaced E_p's, $E_p(5,7)$ and $E_p(6,11)$. Perhaps the two support each other creating an extra strong resonance over the width of the three gaps, which then creates the gaps with the material in the gaps evolving into the two ringlets and Pan.

Similar considerations lead to the assignment of $E_p(7,\infty)$ to the inner and outer edges of the C ring just as it is assigned to the inner edge of the A ring. With these points, the PED in Fig. 13 starts to take shape. The PED rises upward from its minimum towards Saturn's surface where it ends at the inner edge of the D ring [29] where $E_p = E_p(6,\infty)$. In Table 8 the series of close E_p's from $E_p(7,20)$ to $E_p(7,\infty)$ and from $E_p(7,29)$ to $E_p(7,\infty)$ create resonances that produces the A ring and C rings respectively. Also the series of close E_p's from $E_p(6,12)$ to $E_p(6,\infty)$ produces the D ring. The C ring is different from the A, D and E rings in that the C ring is centered at the center of the dip in the PED in the Saturnian disk. Therefore *both* of the C ring's edges are associated with a photon series limit, $E_p(7,\infty)$. Also, because the B ring is at the peak in the PED, neither of its edges are associated with a photon series limit.

The radii of the ringlets D68, D72 and D73 in Saturn's D ring were determined (Hedman et al. 2007b) from Cassini spacecraft images. These ringlets, with indices [26], [27] and [28], and the inner and outer